PCCP

PAPER

View Article Online
View Journal | View Issue

Cite this: *Phys. Chem. Chem. Phys.*, 2014, **16**, 17786

Enhanced photoluminescence and photoactivity of plasmon sensitized nSiNWs/TiO_2 heterostructures†

Sandeep G. Yenchalwar,[ab] Vedi Kuyil Azhagan[a] and Manjusha V. Shelke*[abc]

Received 7th April 2014,
Accepted 5th June 2014

DOI: 10.1039/c4cp01497a

www.rsc.org/pccp

A light sensitive wide band gap radial heterojunction between TiO_2 and nSiNWs sensitized by gold nanoparticles is reported. The surface plasmon of AuNPs influences the optical and photocurrent properties of the heterojunction considerably. Improvement in the band gap emission of TiO_2 has been found at the expense of defect radiation. Excitation of AuNPs deposited on nSiNWs/TiO_2 by light irradiation shows a wavelength-dependent photocurrent due to the increased photoactivity of the heterojunction.

Light detection and photocurrent generation from the excitation of surface plasmon on the surface of metal nanoparticles is a recent concept. There has been a profound surge of interest in exploiting the collective oscillations of the conduction electrons of a metal as a powerful method for use in nanoscience and nanotechnology. Metal nanoparticles exhibit localized surface plasmon resonance (LSPR) by the interaction of visible-light photons with the valence electrons on the metal surface. At a resonance frequency of metal nanoparticles the strongest optical interaction occurs being a function of the size, shape, type of metals as well as the local dielectric environment.[1,2] The large resonant scattering cross sections of metal nanostructures offer the potential to scatter light strongly, while LSPs can guide and confine light flux in nanoscale dimensions.[3] The LSPs decay radiatively by scattering or non-radiatively resulting in energy absorption.[4] These tunable properties of metal nanoparticles can be used in a variety of applications from non-linear optics and photovoltaics to sensing.[5–7]

Due to their versatile properties and easy, controllable synthesis, silicon nanowires (SiNWs) are important candidates for optoelectronic devices and solar cells.[8,9] One-dimensional SiNW arrays offer increased surface area, enhanced light absorption and reduced charge recombination. Oxides with wide band gaps and high dielectric constants, commonly known as *k*-oxides, are of great interest in the electronic industry. TiO_2 is a remarkable semiconductor material with a large band gap (3.0–3.2 eV), is chemically inert, has a high photo-conversion efficiency and good photo-stability.[10,11] Although Si is more efficient, it corrodes in water, and the large band gap of TiO_2 restricts its applications in certain requirements, *e.g.* water splitting in the visible part of the spectrum. Semiconductor heterojunctions are being studied to overcome these shortcomings. The performance of functional devices in water splitting applications is based on the heterojunctions formed between TiO_2 and silicon. Such heterojunctions allow effective separation and utilization of charge carriers (e^-/h^+) by increased absorption of light. Band bending near the junction of nSiNWs/TiO_2 for photo-oxidative properties of the hybrid in photoelectrochemical cells has been studied, where it has been observed that the photocurrent increases due to enhanced charge separation and minimum recombination.[12] Photocatalytic degradation of phenol on an electrode with n–n and p–n heterojunctions has been observed between SiNWs and TiO_2.[13] Semiconductor–metal composites are highly valued for their visible light sensitivity because of the plasmonic antenna effect of metal nanoparticles extending the absorption range of wide band gap semiconductors. Such hybrid nanomaterials show enhanced physical properties such as low reflection, high absorption, dielectric strength *etc.*

In this work, we demonstrate the effect of the surface plasmon of gold nanoparticles on SiNWs/TiO_2 heterojunctions. These hybrids show enhanced optical absorption, emission and photocurrent generation. Plasmonic sensitization enhances self-trapped exciton emission and oxygen vacancy radiative recombination emission properties of TiO_2. Light-emitting diodes (LEDs) are used as a source of light for photocurrent measurements. Enhanced photocurrent is achieved by decorating AuNPs on the surface of nSiNWs/TiO_2 heterojunctions due to plasmonic charge carrier generation.

[a] *Physical and Materials Chemistry Division, CSIR-National Chemical Laboratory, Pune-411008, MH, India. E-mail: shelkemanju@gmail.com*
[b] *Academy of Scientific and Innovative Research (AcSIR), AnusandhanBhawan, 2 Rafi Marg, New Delhi-110001, India*
[c] *CSIR-Network Institute of Solar Energy, CSIR-National Chemical Laboratory, Pune-411008, MH, India*

† Electronic supplementary information (ESI) available: Experimental methods, EDAX analysis spectrum. See DOI: 10.1039/c4cp01497a

Result and discussion

The as-prepared heterojunction materials were characterized by SEM. Fig. 1a and b show the images of vertical SiNWs of approximately 3 μm in length and 100 nm in diameter. It can be seen in Fig. 1b that the individual Si nanowires are uniformly covered by the TiO_2 layer. Fig. 1c and d show the HRTEM images of the same SiNWs/TiO_2 sample; the thickness of the TiO_2 layer is ~20 nm with 8.6 nm (~9 nm)-sized gold nanoparticles on its surface, suggesting the effectiveness of the process utilized herein for the synthesis of the hybrids. The nanoparticles are found to be buried in the TiO_2 matrix because during the synthesis, samples were soaked in a gold salt solution where Au(III) ions may have percolated through the TiO_2 layer.

Fig. 2a shows the typical XRD pattern of the gold nanoparticle-decorated radial heterojunction of SiNWs/TiO_2. The peaks at 2θ = 32.2 (100) and 69.3 (400) correspond to the highly crystalline nature of SiNWs. The peaks appearing at 25.4 (101), and 75.3 (215) belong to the crystalline anatase phase of the TiO_2 [JCPDS No. 841285]. New peaks at 38.2 and 44.4 represent (100) and (200) orientations of face-centered cubic symmetry of the gold nanoparticles [JCPDS No. 040784].

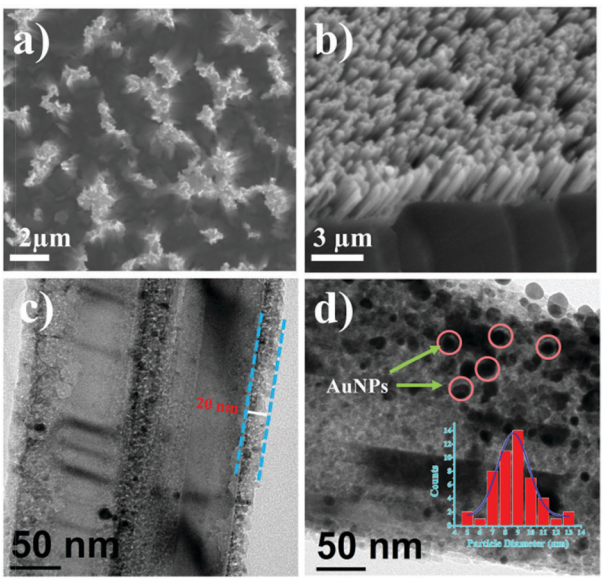

Fig. 1 (a) Top view and (b) cross section (tilt at 45°) SEM views of the as-prepared nSiNWs/TiO_2 heterojunction. (c, d) HRTEM images of the TiO_2-coated nSiNWs before and after gold nanoparticle deposition, respectively.

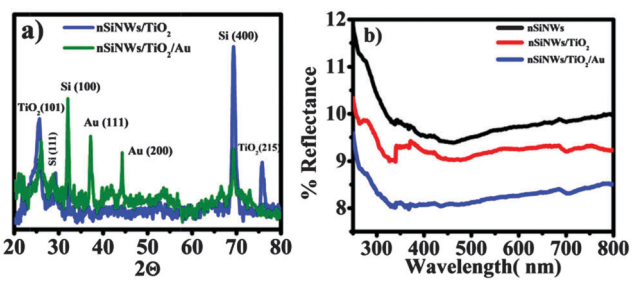

Fig. 2 (a) X-Ray diffraction pattern showing the anatase form of the thin TiO_2 overlayer along with typical gold lattice planes. (b) Comparative diffuse reflectance spectra of the as-prepared samples.

Diffuse reflectance spectra (Fig. 2b) were recorded for the pristine SiNWs, TiO_2-coated SiNWs and Au nanoparticle-decorated SiNWs/TiO_2 samples. All samples show lower reflectance over the spectral range of 300–800 nm than the silicon. This reveals the increased light harvesting capability of heterojunctions compared to pristine SiNWs. The thin TiO_2 layer on the SiNWs acts as a surface passivating layer as well as an anti-reflection coating, improving the absorbance by multiple internal reflections.

The heterojunction can utilize light from both the visible and UV regions of the electromagnetic spectrum, which remarkably enhances its properties towards potential applications. The TiO_2-coated SiNWs samples show ~8% reflectance over the entire visible range after the embedding of gold nanoparticles in the TiO_2 matrix, including the interband transition of SiNWs and TiO_2. Also, an increase in absorption in the range of 450–550 nm is due to the surface plasmon of the gold nanoparticles. Mechanisms such as (i) a change in the refractive index of the metal oxide (here TiO_2) due to the embedded gold nanoparticles or (ii) a change in the effective electron density of the AuNPs could be responsible for the broad nature of the peak. Deposition of AuNPs on the TiO_2 overlayer further enhances light absorption. This is possibly due to LSPRs caused by the light interactions, which increase the scattering ability of AuNPs in a medium of higher refractive index, leading to more photon absorption.[14]

Raman scattering is a sensitive technique to probe lattice microstructures and vibrations. Raman spectra (Fig. 3a) display the crystallinity of SiNWs and TiO_2 and moreover suggest the strain induced by the thin-layer coating of TiO_2 on SiNWs and the disordered or rough surface of the SiNWs. The sharp peaks at 145.60 cm^{-1} and 636.96 cm^{-1} belong to the optical vibration E_g modes in anatase TiO_2.[15] The peak at 520.13 cm^{-1}, which is characteristic of crystalline silicon, arises from the scattering of incident light by the first order longitudinal and transversal optical phonon (LTO) in the diamond structures of SiNWs. The peak at 303.86 cm^{-1} is the second order transverse acoustic phonon (2TA) contribution, which appears to be significant in the spectra.[16,17] The selection rule does not allow this band to appear in normal crystalline Si, but this rule is broken in the disordered material. The band for the E_g mode is further enhanced after the deposition of AuNPs, and a small shift of 1 cm^{-1} is observed. The broad band centered at 960.1 cm^{-1} is related to second order transversal optical phonons (2TO) in silicon, and also suggests a strong interaction between the TiO_2 thin film and the silicon surface. The peak at 855.8 cm^{-1} could be ascribed to a Ti–O–Ti stretch, indicating 2D connectivity.[18]

Solid state photoluminescence (PL) spectroscopy was used to understand the presence of defects and the recombination ability of charge carriers. Room temperature photoluminescence spectra have been plotted in Fig. 3b. The as-prepared samples were excited at the band edge absorption of the TiO_2, *i.e.* 340 nm. Both samples show multi-emission peaks which have been de-convoluted using Gaussian fitting in order to understand their peak positions and nature. For semiconductors such as TiO_2 and ZnO, on excitation by a photon energy equal to or

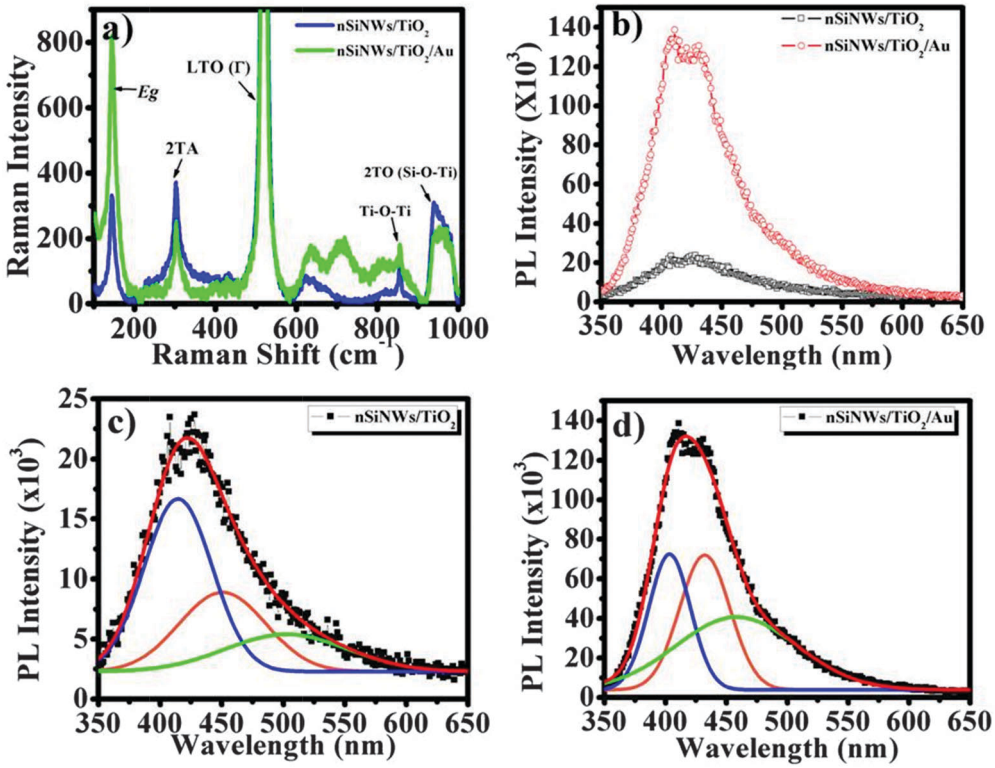

Fig. 3 (a) Micro-Raman spectra before and after deposition of AuNPs on the nSiNWs/TiO_2 heterojunction, indicating the typical anatase peak of TiO_2 and first and second order silicon peaks. (b) Room temperature photoluminescence spectra of the heterojunctions. (c, d) Gaussian fitted PL peaks of the as-prepared samples before and after AuNPs deposition, respectively.

higher than their band gap, electrons can be transferred from the valence band to the conduction band, generating excitons which after recombining emit radiation approximately equal in energy to the band gap. However, this is not always true, since the presence of defects such as oxygen deficiencies, impurities or metal doping creates sub-energy levels that can capture the electrons, resulting in emission of photons lower in energy than the band gap. The oxygen-related defects in TiO_2 are intrinsic and particularly important as they give rise to intermediate energy levels within the band gap. As a consequence, many recombination centers are introduced for electron–hole pairs.

In the absence of gold nanoparticles, TiO_2 shows PL peaks at 415 nm, 451 nm and 503 nm (Fig. 3c), which belong to self-trapped excitons (STEs), oxygen vacancies with two electrons (F-center or $V_O^{\bullet\bullet}$) and oxygen vacancies with one electron ($V_O^{\bullet}$), respectively. After gold nanoparticle deposition (Fig. 3d), new peaks appeared at 403 nm, 433 nm and 458 nm. All these peaks confirm the anatase-type TiO_2 thin layer formed on the SiNWs. The PL of anatase TiO_2 has three different physical origins, namely radiative recombination of self-trapped excitons, oxygen vacancies (OVs), and surface states[19] in the defect states within the band gap. It has been reported that oxygen vacancies in metal oxides behave as deep trap states which enhance the recombination of charge carriers, and shallow trap states promote diffusion of carriers to the surface.[20,21]

The mechanism for the PL in TiO_2 can be described by the following processes:[19]

$$TiO_2 \xrightarrow{h\nu} TiO_2(e^- + h^+) \rightarrow e^-_{CB} + h^+_{VB}$$

$$V_O^{\bullet} + e^-_{CB} \rightarrow V_O \text{ (shallow state trapped electrons)}$$

$$V_O + h^+_{VB} \rightarrow V_O^{\bullet} + h\nu \text{ (radiative recombination)}$$

where $V_O^{\bullet}$ is a Kroger notation for the ionized oxygen vacancy level.

The conduction and valence band edges for titanium oxide lie at ~4.26 eV and ~7.46 eV with respect to the vacuum, considering the anatase TiO_2 band gap of 3.2 eV.[22] The shallow traps belonging to oxygen vacancies were established to be 0.51 eV[19] and 0.8 eV[23] below the conduction band. The peaks at 451 nm and 503 nm in Fig. 3c are nearly coincident with these OV levels.

The electrons excited from the valence band (VB) of the TiO_2 cannot reach the conduction band (CB) of TiO_2; instead they are captured by the oxygen vacancies *via* a non-radiative process and then recombine with the holes in the VB, accompanying radiative emission in the visible region corresponding to the peak at 415 nm. A blue shift of 12 nm in the band edge luminescence is observed for the gold-deposited samples, suggesting trapping of electrons in the energy level just below the CB of TiO_2. It also emphasizes the strong interfacial

interaction between TiO_2 and gold nanoparticles. The emission at 432 nm corresponds to self-trapped excitons (STE), which have been suggested to occur due to oxygen vacancies created by metal doping (here by Au metal).[24,25] The considerably increased intensity of shallow trap states after the deposition of gold nanoparticles infers increased radiative recombination at this level. The photoluminescence of the heterojunction on gold deposition shows a 5-fold enhancement after integrating the emission signals of TiO_2. This suggests that the rate of semiconductor emission in a gold nanoparticle-decorated heterojunction system, which is a function of the concentration of electron–hole pairs in the semiconductor, is larger than that in the isolated heterojunction system. This can be explained only by the involvement of SPR of AuNPs, which increases the rate of electron–hole pair formation in the semiconductor due to a near-field effect. The photoexcited plasmonic AuNPs efficiently scatter resonant photons, increasing the average photon path-length in the TiO_2 layer and ultimately resulting in an enhanced rate of exciton formation. More precisely, the defect emission energy (503 nm) is close to the SPR of gold nanoparticles as per the DRS spectra. This energy is absorbed by the gold nanoparticles, generating energetic electrons (hot electrons) in the high energy state within the Fermi level, which could be transferred from the gold nanoparticles into the conduction band of the TiO_2. After this, by combining with the holes in the VB of the TiO_2, relaxation occurs by emission of energetic photons, which results in an increase in the intensity of the other emission band of TiO_2.[26,27]

To investigate the effect of the increased absorption and PL caused by the gold nanoparticles on the photocurrent, we carried out photocurrent measurements. Spectrally resolved photoelectrochemical behavior of the samples was studied in a neutral medium using Na_2SO_4 solution under LED light illumination. Both electrodes were photoactive to the LED light irradiation. Fig. 4A shows the linear sweep voltammograms before and after gold nanoparticle deposition on the heterojunction, recorded in the potential range between −1 to +2 V, with Ag/AgCl as a reference electrode, under dark and white light illumination and with a scan rate of 100 mV s^{-1}. Both the samples show a pronounced photocurrent over the dark current, but the photocurrent is substantially higher for gold nanoparticle-decorated samples, as evident from the graph. The dependence of the photocurrent on the time of illumination at the applied potential (0.5 V *vs.* Ag/AgCl) is shown in Fig. 4B.

The SiNWs/TiO_2 heterojunction shows a maximum photocurrent of 0.33 μA cm^{-2} under white light illumination due to enhanced absorption of the visible light over SiNWs and favorable band alignment for the possible photoexcited electron transfer. Photoelectrodes with AuNPs show an approximate 25-fold enhancement in the photocurrent (~8.4 μA cm^{-2}). This increment in the current can be attributed to the possible role of the gold nanoparticles, as these enhance the other physical properties of the heterojunction as discussed above. In order to establish the role of the gold nanoparticles in the photocurrent enhancement, a wavelength-dependent study was carried out and the results are presented in Fig. 5A and B. When irradiated by a green LED light (central wavelength at 530 nm, total power output ~22.3 mW cm^{-2}) with an incident power of 11.2 mW on the prescribed area of the electrode, *i.e.* 0.5 cm × 0.5 cm, the highest current is obtained as compared to the other wavelengths.

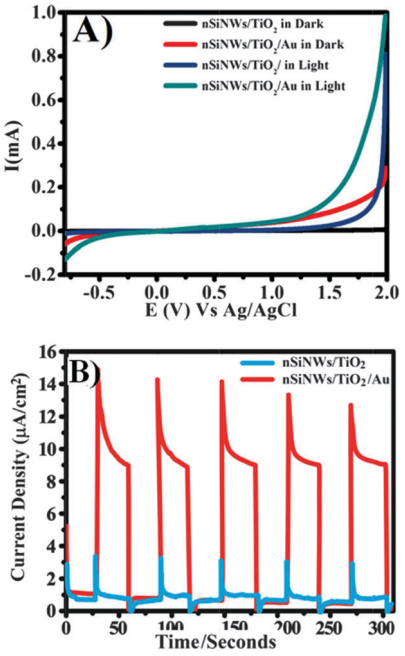

Fig. 4 (A) Linear sweep voltammograms (LSVs) and (B) transient photocurrent of the nSiNWs/TiO_2 and nSiNWs/TiO_2/Au samples under dark and white light illumination under the bias of 0.5 V *vs.* Ag/AgCl. The gold-decorated nSiNWs/TiO_2 heterojunction shows the highest photocurrent due to increased visible light absorption.

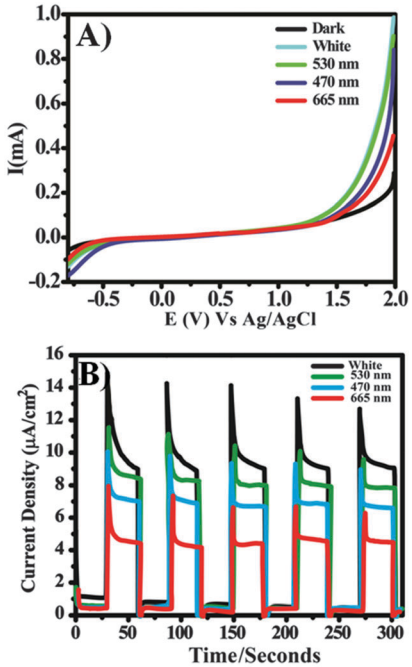

Fig. 5 (A) LSVs and (B) wavelength-dependent photoresponse of the nSiNWs/TiO_2/Au. All measurements were carried out with a bias of 0.5 V *vs.* Ag/AgCl, with 1 M Na_2SO_4 as the electrolyte.

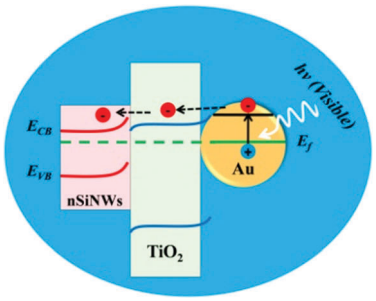

Scheme 1 Simplified illustration of the band energies and possible charge transfer from the gold nanoparticle SPR level into the conduction band of TiO_2 under visible light illumination.

The gold deposited on the heterojunction has a maximum absorbance in the region of 400–550 nm, which is due to the combined effect of SPR and the dielectric strength of the TiO_2. Therefore, it is reasonable to assume that the photocurrent response at 470 nm ($\sim$6.43 μA cm^{-2}) and 530 nm ($\sim$7.8 μA cm^{-2}) is because of the spectral overlap of the energy levels of the SPR of the gold nanoparticles and TiO_2. The photon energy (530 nm) is selectively absorbed by the gold nanoparticles over the highly energetic photons (470 nm) and hence the maximum photocurrent is observed under green light irradiation. The absorbance of the gold-decorated samples extends over the entire visible region, hence it should be able to convert incident photons of 665 nm wavelength as well, resulting in the higher photocurrent ($\sim$4.14 μA cm^{-2}) at this wavelength.

To produce photocurrent from the gold nanoparticle-decorated nSiNWs/TiO_2, the electrons and holes must have to be transferred across the heterojunction (Scheme 1).

A barrier of 1.1 eV exists between the AuNPs–TiO_2 interface because of the difference in the work function of gold ($\sim$5 eV) and the electron affinity of TiO_2 ($\sim$3.9 eV)[28], which has to be overcome by the electrons so as to contribute to the current.

As the present study suggests, the increase in the photocurrent on visible light irradiation indicates that these electrons have enough energy to cross the Schottky barrier. Also, SPRs on gold can be stimulated by the defect emission ($\sim$2.5 eV) energy transfer. The excited SPRs might be responsible for the electron tunneling from gold to the TiO_2 conduction band. As a result, electron density increases in the conduction band of TiO_2, leading to a higher recombination rate of electron–hole pairs, which enhances the PL properties of TiO_2. All of this suggests a synergistic effect between TiO_2 emission and gold SPR involvement in the enhanced photoactivity of the heterojunction.

Conclusions

A simple method has been presented for the synthesis of heterojunctions, along with improved and new properties of such heterojunctions resulting from deposition of gold nanoparticles. The influence of the SPR of gold nanoparticles on the optical and photocurrent properties of the nSiNWs/TiO_2 heterojunction has been investigated. Such gold plasmon-sensitized SiNWs/TiO_2 exhibits broadband visible light absorbance and photoresponse at matching wavelengths between the SPR and interband transitions. The enhanced absorption, enhanced rate of electron–hole pair formation, electric field amplification and simultaneous plasmonic energy transfer to the semiconductor is attributed to the increased response towards the multi-wavelength photoconductivity of the heterojunction. The deposition of noble metal nanoparticles on semiconductors or semiconductor heterojunctions can be effectively used in the preparation of highly efficient optoelectronic devices.

Acknowledgements

SGY acknowledges a research fellowship from UGC. This work is supported by the Council of Scientific and Industrial Research (CSIR), India through the TAPSUN program.

References

1 K. L. Kelly, E. Coronado, L. L. Zhao and G. C. Schatz, *J. Phys. Chem. B*, 2003, **107**, 668.
2 L. Gunnarsson, *J. Phys. Chem. B*, 2005, **109**, 1079.
3 J. A. Schuller, E. S. Barnard, W. Cai, Y. C. Jun, J. S. White and M. L. Brongersma, *Nat. Mater.*, 2010, **9**, 193.
4 M. Kauranen and A. V. Zayats, *Nat. Photonics*, 2012, **6**, 737.
5 H. A. Atwater and A. Polman, *Nat. Mater.*, 2010, **9**, 205.
6 S. Nie and S. R. Emory, *Science*, 1997, **275**, 1102.
7 S. Kühn, U. Håkanson, L. Rogobete and V. Sandoghdar, *Phys. Rev. Lett.*, 2006, **97**, 017402.
8 B. Tian, X. Zheng, T. J. Kempa, Y. Fang, N. Yu, G. Yu, J. Huang and C. M. Lieber, *Nat. Mater.*, 2007, **449**, 885.
9 I. Hochbaum, R. Chen, R. D. Delgado, W. Liang, E. C. Garnett, M. Najarian, A. Majumdar and P. Yang, *Nat. Mater.*, 2008, **451**, 163.
10 X. Chen and S. S. Mao, *Chem. Rev.*, 2007, **107**, 2891.
11 R. Asahi, T. Morikawa, T. Ohwaki, K. Aoki and Y. Taga, *Science*, 2001, **293**, 269.
12 Y. J. Hwang, A. Boukai and P. Yang, *Nano Lett.*, 2009, **9**, 410.
13 H. Yu, X. Li, X. Quan, S. Chen and Y. Zhang, *Environ. Sci. Technol.*, 2009, **43**, 7849.
14 K. R. Catchpole and A. Polman, *Opt. Express*, 2008, **16**, 21793.
15 D. Bersani, P. P. Lottici and X.-Z. Ding, *Appl. Phys. Lett.*, 1998, **72**, 73.
16 R. Wang, G. Zhou, Y. Liu, S. Pan, H. Zhang, D. Yu and Z. Zhang, *Phys. Rev. B: Condens. Matter Mater. Phys.*, 2000, **61**, 16827.
17 B. Li, D. Yu and S. L. Zhang, *Phys. Rev. B: Condens. Matter Mater. Phys.*, 1999, **59**, 1645.
18 M. Fernández-García, X. Wang, C. Belver, J. C. Hanson and J. A. Rodriguez, *J. Phys. Chem. C*, 2007, **111**, 674.
19 N. Serpone, D. Lawless and R. Khairutdinovt, *J. Phys. Chem.*, 1995, **99**, 16646.
20 Y. Lei, L. D. Zhang, G. W. Meng, G. H. Li and X. Y. Zhang, *Appl. Phys. Lett.*, 2001, **78**, 1125.

21 G. Mattioli, F. Filippone, P. Alippi and A. M. Bonapasta, *Phys. Rev. B: Condens. Matter Mater. Phys.*, 2008, **78**, 241201.
22 I. Chung, B. Lee, J. He, R. P. H. Chang and M. G. Kanatzidis, *Nature*, 2012, **485**, 486.
23 L. V. Saraf, S. I. Patil, S. B. Ogale, S. R. Sainkar and S. T. Kshirsager, *Int. J. Mod. Phys. B*, 1998, **12**, 2635.
24 K. Iijima, M. Goto, S. Enomoto, H. Kunugita, K. Ema, M. Tsukamoto, N. Ichikawa and H. Sakama, *J. Lumin.*, 2008, **128**, 911.
25 B. Choudhury, M. Dey and A. Choudhury, *Appl. Nanosci.*, 2013, **4**, 499.
26 C. W. Cheng, E. J. Sie, B. Liu, C. H. A. Huan, T. C. Sum, H. D. Sun and H. J. Fan, *Appl. Phys. Lett.*, 2010, **96**, 071107.
27 H. Y. Lin, C. L. Cheng, Y. Y. Chou, L. L. Huang and Y. F. Chen, *Opt. Express*, 2006, **14**, 2372.
28 G. Rothenberger, D. Fitzmaurice and M. Gratzel, *J. Phys. Chem.*, 1992, **96**, 5983.